Bioorganic & Medicinal Chemistry 18 (2010) 7639–7650

Contents lists available at ScienceDirect

Bioorganic & Medicinal Chemistry

journal homepage: www.elsevier.com/locate/bmc

A convenient synthesis and molecular modeling study of novel purine and pyrimidine derivatives as CDK2/cyclin A3 inhibitors

Abdel-Sattar S. Hamad Elgazwy [a,*], Nasser S. M. Ismail [b], Heba S. A. Elzahabi [c]

[a] Department of Chemistry, Faculty of Science, University of Ain Shams, Abbassia 11566, Cairo, Egypt
[b] Department of Pharmaceutical Chemistry, Faculty of Pharmacy University of Ain Shams, Abbassia 11566, Cairo, Egypt
[c] Department of Pharmaceutical Chemistry, Faculty of Pharmacy (Girls Branch), Al azahar University, Nasser City, Cairo, Egypt

ARTICLE INFO

Article history:
Received 27 June 2010
Revised 10 August 2010
Accepted 16 August 2010
Available online 26 August 2010

Keywords:
Diaminomaleonitrile (DAMN)
Purine
Pyrimidine
CDK2
Molecular modeling
Antitumor
Docking
Bioinformatics

ABSTRACT

A series of novel purine and pyrimidine derivatives were prepared and biologically evaluated for their in vitro anti-CDK2/cyclin A3 and antitumor activities in Ehrlich ascites carcinoma (EAC) cell based assay. The novel purine derivatives **13a,b** demonstrated potent inhibitor activities with IC_{50} values of 14 ± 9 and 13 ± 9 μM, respectively. Additionally, compound **15a** showed the highest potency (IC_{50} = 10 ± 6 μM) in EAC cell based assay. Molecular modeling study, including fitting to a 3D-pharmacophore model and their docking into cyclin dependant kinase2 (CDK2) active site showed high fit values and docking scores.

1. Introduction

Diaminomaleonitrile (DAMN) and its N-substituted derivatives are very useful compounds in heterocyclic synthesis.[1–6] During the course of our investigations on the use of DAMN in heterocyclic synthesis, we have designed new approaches to 4-cyano-1,3-dihydro-2-oxo-2*H*-imidazole-5-(N^1-tosyl)carboxamide **11** (Scheme 1) as a reactive precursor of thiopurine.[7] In some of these cases, new DAMN derivatives and *N*-({[(*Z*)-2-amino-1,2-dicyanovinyl]-amino}carbonyl)-4-methylbenzenesulfonamide **10**, were used as key intermediates and we give herein a report on these compounds in more detail. Recently, there has been described various natural manifestations of purine systems, that is, methylated, higher-alkylated, and glycosylated forms.[8] These comprise the purine alkaloids, cytokinines, as well as the purine nucleoside antibiotics. In part, the compounds described were isolated from natural sources already long ago. However, some have been reported only during the last few years. In brief, the biological activities of most of the purine derivatives are briefly described[9] as potential anticancer, anti-HIV-1, antimicrobial agents and in some cases, syntheses are formulated.

In particular, this article introduces the main synthetic principles for the generation of the purine ring system and 2,6,9-trisubstituted purines as inhibitors of cyclin/CDK complexes.[10] Also, these compounds are potent inhibitors of human cellular proliferation. They are useful in treating a disorder mediated by elevated levels of cell proliferation in a mammal compared to a healthy one by administering an effective dose. In the treatment of proliferative diseases the interruption of the cell cycle is one approach. The phases of the cell cycle are driven by cyclin-dependent kinases.[11–15] Upon complexation with its activating proteins, cyclin E or cyclin A, cycline-dependent kinase2 (CDK2) modulates the activity of many cellular substrates via phosphorylation on Ser and/or Thr residues.[16] In complex with cyclin E, cycline-dependent kinase2 (CDK2) plays a paramount role during the G1/S transition of the cell cycle while in complex with cyclin A, it facilitates the progression of the S phase of the cell cycle. Recent evidence also suggests that CDK2 may have a crucial role in the G2 phase of the cell cycle.[17,18] The importance of cycline-dependent kinase2 (CDK2) for cell cycle progression has led to an active pursuit of small molecule inhibitors of this enzyme as a possible treatment against cancer and other hyper-proliferative disorders.[19] Our current investigation was based on; first, using a structure-guided strategy based on cycline-dependent kinase2 (CDK2)[20–26] was as appropriate means to generate CDK2 inhibitors that might prove useful for the therapy of proliferative disorders.

* Corresponding author. Tel.: +202 26173044; fax: +202 24831836.
E-mail addresses: aselgazwy@yahoo.com, elgazwy@sci.asu.edu.eg, elgazwy@usa.com (Abdel-Sattar S. Hamad Elgazwy).

0968-0896/$ - see front matter © 2010 Elsevier Ltd. All rights reserved.
doi:10.1016/j.bmc.2010.08.033

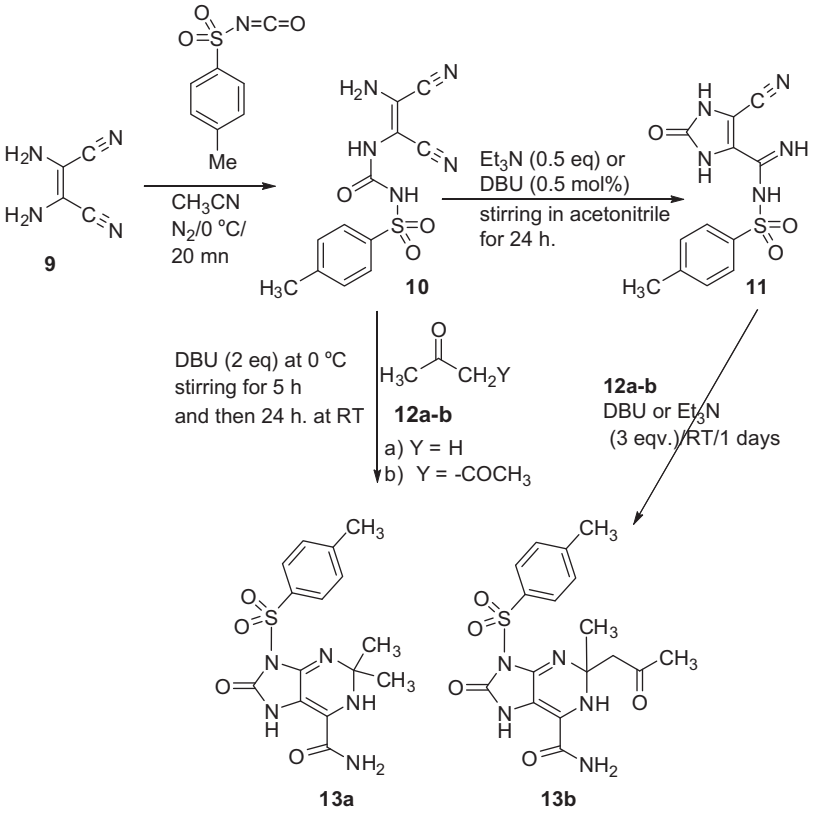

Scheme 1.

Several cores have been reported as potent CDK inhibitors including purines, pyrimidine and quinazolines (Fig. 1).[27–30] It has previously been found that the presence of hetero-bicyclic ring systems was essential to gain access to the phosphate binding region of the ATP-kinases pocket.

Second, the molecular modeling work on the cycline-dependent kinase2 (CDK2) in complex with ligand (**5**) suggested a binding mode (Fig. 2), where the bicyclic system was located in the ATP binding site, making polar interactions with the kinase binding motif. A large number of crystal structures were available for human CDK2 in complex with small ligands which bind deeply within the ATP site, and which interact with the kinase motif, of particular interest for the purine ring system, the CDK2 complex with ligand **5** (PDB code: 1H0V) is available from the PDB.[30] This example demonstrates the successful use of the fully active cyclin complex in a prospective drug design program.

2. Results and discussion

2.1. Chemistry

The design and synthesis of monosubstituted and disubstituted pyrimidine, urea, purine and annelated imidazole derivatives with anticancer activity are described.[31] N-Alkylation with various side

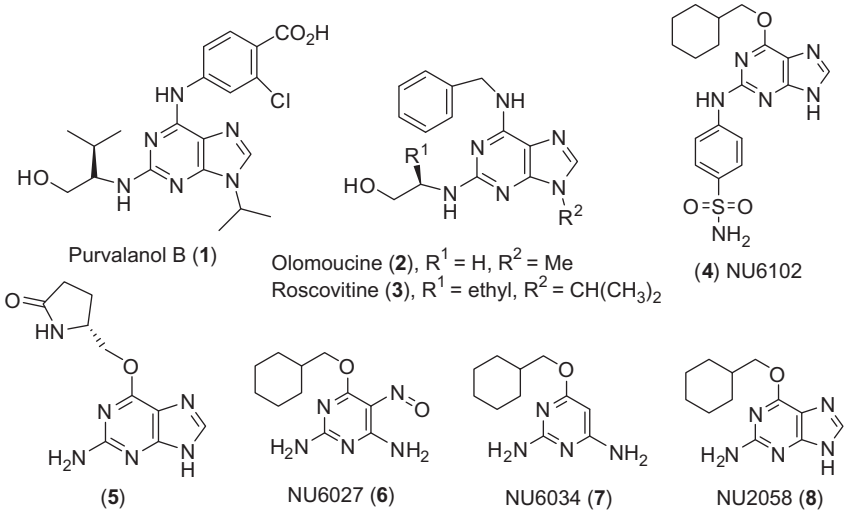

Figure 1. Chemical structures of potent cycline-dependent kinase2 (CDK2) inhibitors.

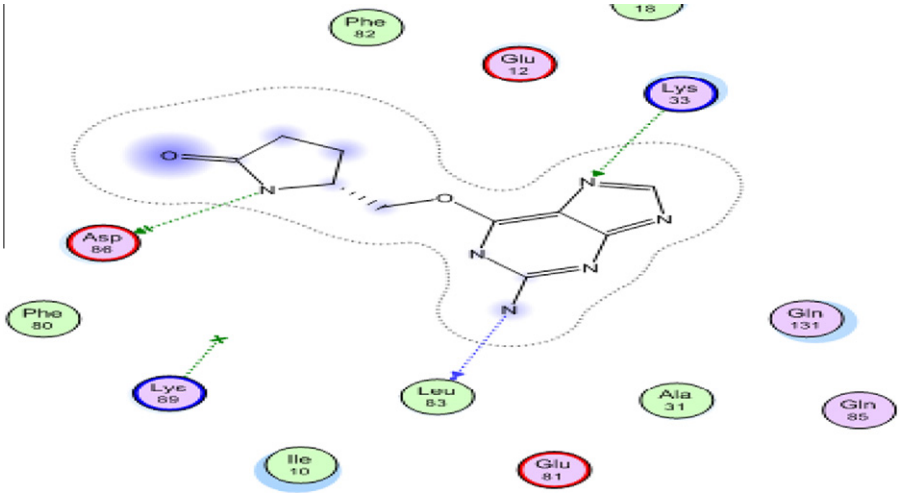

Figure 2. 2D interaction diagram of ligand (**5**) with CDK2 enzyme represented using MOE program with the essential amino acid residues at the binding site are tagged in circles.

chains in the imidazole and pyrimidine rings led to a series of monosubstituted purine products. For preparation of disubstituted purine derivatives, appropriately substituted tosyl isocyanides were used. The biological activity of all the compounds was evaluated against a number of cancer cell lines. The sequence of reactions followed in the synthesis of the target compounds is illustrated in Scheme 1.

This paper described a facile one step synthesis of urea derivative **10**, which was cyclized using a catalytic amount of DBU in acetonitrile to give **11** in fairly high yield (93%). Compounds **10** and **11** were versatile precursors for fused nitrogen heterocycles, especially purine[8] or thiopurine ring.[7] The formation of **11** can be envisaged through the mechanism described by Ernst Schaumann et al.[32] and us,[7] The mechanism illustrated that compound **11** is afforded via rearrangement upon base catalyzed cyclization, as outlined in Scheme 2.

In our research group, we are interested in studying the reactivity of the isolated urea derivatives **10**. For example, treating **10** with aldehydes or ketones in the presence of a base such as DBU (1,8-diazabicyclo[5.4.0]undec-7-ene) or Et_3N (triethylamine) either in catalytic or equivalent amount. A previous detailed study[33] of the reaction of DAMN with isocyanates together with either an aldehyde or ketone in the presence of triethylamine reported that the products of these reactions were pyrimidino[5,4-*d*]pyrimidines. Similarly, we have studied the reaction of **10** with ketone **12** or aldehyde **14** derivatives in the presence of a base as outlined in Schemes 3 and 4, respectively. This reaction takes place either via pathway A or B.

In pathway A, double bond isomerization is proposed under base catalysis during the condensation of **10** with ketone. Intermediate **E** could not be isolated and this was attributed to its rapid cyclization to pyrimidine **F** or its tautomer **G** and subsequent cyclization followed by oxidation in air to give the isolated product, assigned structure **13a,b**. The same product is also obtained from intermediate **F** after prolonged hydrolysis of the cyano group using hydrogen peroxide in acetic acid.

In pathway B, we are unable to isolate the proposed intermediate **A** (Scheme 3). In the presence of base, it was postulated[33] that isomerization occurs around the C=C bond to give an intermediate **C**, which cyclized rapidly to **13a,b**; intermediate **C** could never be isolated.

It can be seen from Scheme 1 that the reaction of DAMN with tosyl isocyanate proceeded was expected to give the urea derivatives **10** in excellent yields. Compound **10** has been previously described by Ohtsuka[33] and our spectroscopic data are in complete agreement with his data and the characteristic nitrile absorption at 2254 and 2210 cm^{-1} and the carbonyl absorption at 1663, 1648 and 1611 cm^{-1} in the IR spectrum. On reaction of **10** with aldehydes or ketones in the presence of triethylamine or DBU at room temperature the products of these reactions were isolated and characterized by physical tools such as IR, ^1H NMR, ^{13}C NMR spectral analysis and allowed us to establish the structures of the products.

The reaction of urea derivatives of DAMN with aldehydes in the presence of DBU or Et_3N, afforded white–pale yellow solids precipitated in good yields. The reaction is inconsistent with the reaction described by Ohtsuka[33] and assigned in pyrimidine structure **16a–d** (in case of aldehyde precursors). We are able to isolate an intermediate **15a–d** which thermally stable in hot acetonitrile and cyclized rapidly to pyrimidine **16a–d**, as shown in Scheme 4.

This article reports on the full assignment of NMR spectra for all products deduced from the correlations established in the 2-D (COSY, HSQC, HMBC) experiments, especially for the imine hydrogen and the spectroscopy results obtained on these compounds products were satisfactory. The ^1H NMR spectrum showed the presence of two broad singlets at δ 6.64 and 9.88 ppm due to the

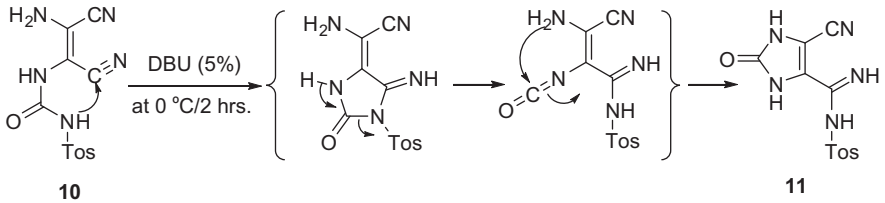

Scheme 2.

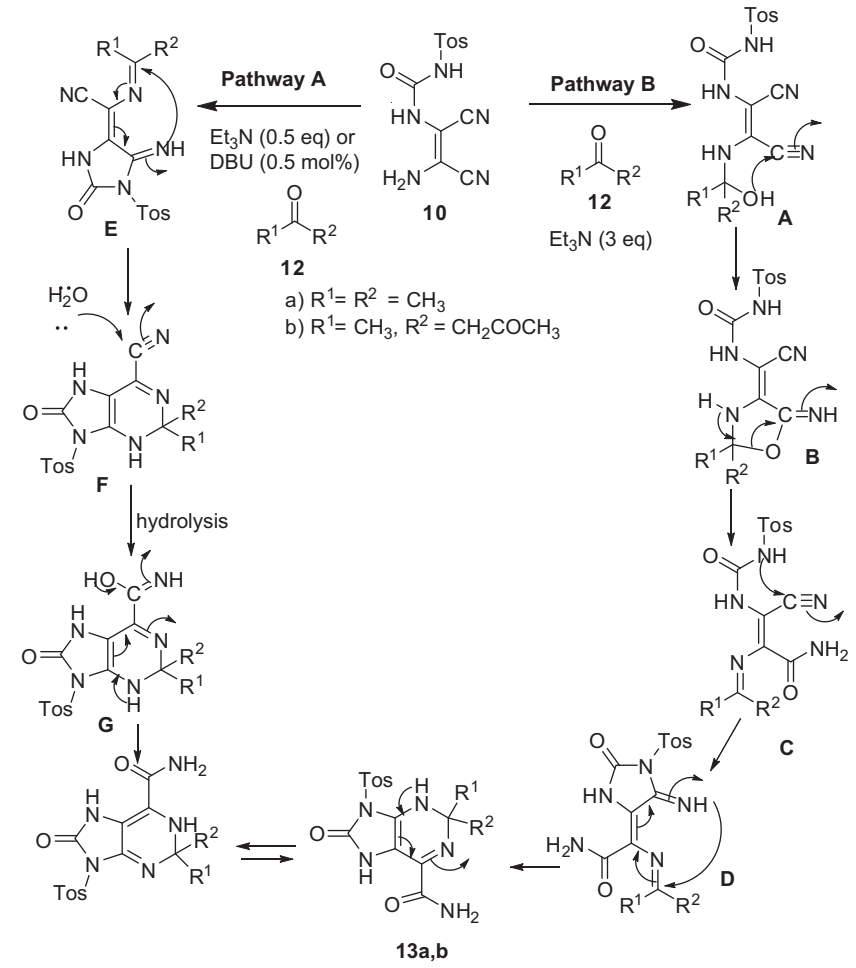

Scheme 3.

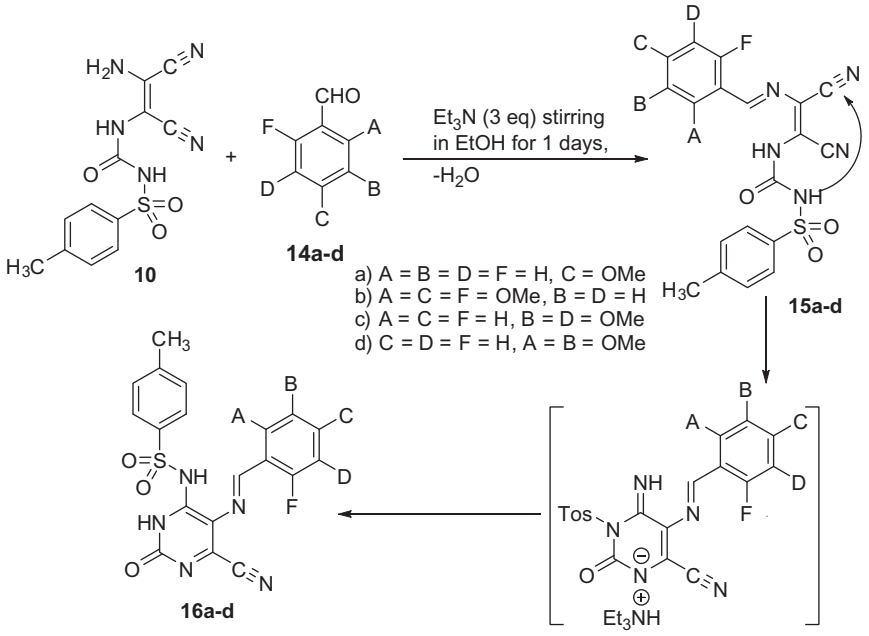

Scheme 4.

amine protons and a singlet at δ 7.28 for the HC proton of the imidazole ring and the ^{13}C NMR spectrum was fully consistent with the assigned structure. The infrared spectrum confirmed the presence of the NH and C=N stretching vibrations within the region of 3420–3160, and 1650–1640 cm^{-1}, respectively. The infrared spectrum also showed a sharp absorption band at 2200–2220 cm^{-1} for

the C≡N stretching vibration. The 8-oxo-6-carboxamido-1,2-dihydropurine **13a,b** was prepared by stirring a suspension of the corresponding urea **10** with a slight excess of acetone or acetylacetone in ethanol at room temperature (Scheme 1). The reactions were monitored by TLC (9:1 $CHCl_3$/EtOH) and reaction times varied between 20 min and 24 h, depending upon the solvent used for the reaction and the rate of precipitation, these 1,2-dihydropurines can be isolated as solids in color from orange to yellow. Compounds **13a,b** were re-crystallized from mixture of ethanol/methanol (1:1) and gave pale yellow to off white crystals, respectively. These were fully characterized by TLC, IR and ^{1}H NMR, ^{13}C NMR and mass spectroscopy. The infrared spectrum confirmed the presence of the NH and C=N stretching vibrations within the region of 3400–3100, and 1660–1650 cm^{-1}, respectively. The C=O of the amide group appeared at 1695–1710 cm^{-1} as a strong band. The high resolution mass spectrum gave a molecular ion peak at 363, 377 $(M+1)^+$. Which fits with the expected molecular weight of 362, 376 for the 1,2-dihydropurine **13a,b**. In the ^{1}H NMR spectra of the isolated compounds **13a** and **13b**, the amide protons were observed in the region of δ 7.69–7.85 ppm and in several cases the assignment were confirmed by D_2O exchange. The H-2 proton appeared as a broad singlet at δ 4.95–4.97 ppm and the aromatic protons showed the expected patterns in the range of δ 6.85–7.30 ppm. The proton of the midazole ring appeared as a sharp singlets in the range of δ 7.42–7.50 ppm. The ^{13}C NMR spectrum of these 1,2-dihydropurine had the expected number of bands, with the C-2 carbon at δ 76.2–76.5, C-4 carbon at δ 136.4–137.2, C-5 carbon at δ 122.2–122.4, C-6 carbon at δ 159.8–160.3, C-8 carbon at δ 148.4–148.7, C=O carbon at δ 166.4–166.8 ppm.

2.2. Biological activity study

The newly synthesized compounds **10, 11, 13a,b, 15a–d, 16a–d** were evaluated in vitro as CDK2/cyclin A3 inhibitors as well as the in vitro study against the viability of EAC cell line.

2.2.1. In vitro CDK2/cyclin A3 inhibition activity

The obtained data (Table 3, Fig. 6) revealed that, we have synthesized some new potent CDK2/cyclin A3 inhibitors, for example, compounds **10**, **13a**,**b** and **16c** comparing to ligand **5**,[30] in particular when the bicyclic purine ring system is held constant, for example, **13a**,**b** (lowest docking and IC_{50} value). Acyclic system of diaminomaleonitrile urea, for example, compound **10**, as well as cyclic pyrimidine derivative, for example, **16c** display lower inhibitory activity than purine derivatives **13a,b**, recording that compound **10** produced higher activity than pyrimidine derivative **16c**. Compound **13a** adopted a preferential binding mode than its acetyl analogue **13b** as well as ligand **5**. Both of the latter compounds illustrated a three hydrogen bond while **13a** adopted four hydrogen bonds (Fig. 5). The purine ring system significantly potentiated the activity of **13a,b** via hydrogen bonding interaction so exerting promising binding mode model, low binding energy together with low IC_{50}. Also, **13a** preferentially formed two hydrogen bonds through its sulfoxide group while that of **13b** analogue formed only one. Also, replacement of (1) hydrogen of methyl group in **13a** by acetyl group producing **13b**, a little bit diminished in vitro cycline-dependent kinase2 (CDK2) inhibitory activity. These could be reasonable explanations for the highest activity exerted by **13a**. Here, diaminomaleonitrile urea derivative **10** is considered as a pivotal compound that is used as a precursor for the synthesis of the other test compounds **11**, **15a–d** and **16a–d**. So that, incorporating the two amino groups in **10** (IC_{50} = 32 μM) into imidazolidinone ring in **11** led to dramatic decrease in CDK2 inhibitory activity (IC_{50} = 45 μM). Also, masking the amino group with different aromatic aldehydes in **15a–d**, reduced the activity (IC_{50} = 38–43 μM). Next, introduction of pyrimidinyl structure in **16a–d**, diversely affect the activity. The recorded data showed that both compounds **15a,b** and their corresponding pyrimidinyl analogues **16a,b**, respectively, displayed the same IC_{50} (Table 3). In these derivatives the OCH_3 substituent of phenyl methylene group oriented in either *para* or *ortho*/*para* direction.

On the other hand, when OCH_3 group takes the *ortho*/*meta* directing group, in this case, the corresponding pyrimidinyl derivatives **16c,d** exerted higher inhibitory activity than their corresponding **15c,d**, respectively, compared to the ligand **5**.

2.2.2. In vitro antitumor activity

Additionally, the target compounds were examined against the viability of EAC cell line, compared to ligand **5** (Table 3). The recorded GI_{50} values revealed that urea derivative **10** significantly showed higher activity than ligand **5**. Introduction of *p*-OCH_3 phenyl methylene moiety to compound **10** (GI_{50} = 12 μM), affording **15a** potentiated the antitumor activity (GI_{50} = 10 μM). It was observed that both diaminomaleonitrile urea derivatives **10** and **15a** possess acyclic skeleton. Also introduction of cyclic skeleton, for example, purine ring system as in **13a,b** or pyrimidinyl moiety as in **16b** showed considerable antitumor activity (GI_{50} = 15–16 μM). Another interesting observation is that purine derivative **13b** as well as pyrimidine derivative **16b** showed the same antitumor activity (GI_{50} = 16 μM). Concerning phenyl methylene derivatives **15a–d**, it was found that **15a** (the most active compound) has only one OCH_3 group in *para* position. Increasing the number of OCH_3 groups and varying their positions, for example, **15b–d** led to a dramatic reduction in the activity. While the *p*-OCH_3 and *s*-tri-OCH_3 substituted phenyl methylene moiety when combined with the cyclic pyrimidine nucleus, for example, **16a,b** showed higher activity than ligand **5**.

2.3. A molecular modeling study

Pharmacophore model was generated using the Discovery Studio 2.5 software (Accelrys Inc., San Diego, CA, USA). Molecular docking into the prepared enzyme was performed using the MOE.

2.3.1. Generation of CDK2 inhibitor hypothesis

The pharmacophore modeling method, as a key tool of computer aided drug design, has been widely used in lead discovery and optimization.[34–36] Hip-Hop algorithm, which identifies common chemical features from a set of ligands without the use of affinity data, was used to develop the pharmacophore model for CDK2 inhibitor. The feature-based pharmacophore model was mapped from a set of highly selective ligands (Fig. 1). The set of conformational models of each structure of the training set was performed using the prepare ligand protocol and was used to generate the common feature hypotheses.

2.3.2. Validation of the generated pharmacophore

Ten hypotheses were generated[37] and the one ranked number 4 was chosen as the valid ideal hypothesis (Fig. 3) based on the following: (a) The hypothesis showed full mapping of all its features without any steric clashes together with high fit values with the training set (compounds **1–8**, e.g., see Fig. 4a), (b) Retrospectively, the simulated fit values of test set compounds (**10, 11, 13a,b, 15a–d, 16a–d**) with hypothesis 4 were more consistent with the experimental results than the others[38] (c) The database search study for examining the affinity of such hypothesis with the molecular structures of MiniMaybridge databases revealed that only 19 hits have been retrieved from the databases (2000 compounds). Such a low number of the recognized database molecules by generated hypothesis may give an additional advantage and selectivity to our hypothesis. Such an ideal hypothesis encompassed four

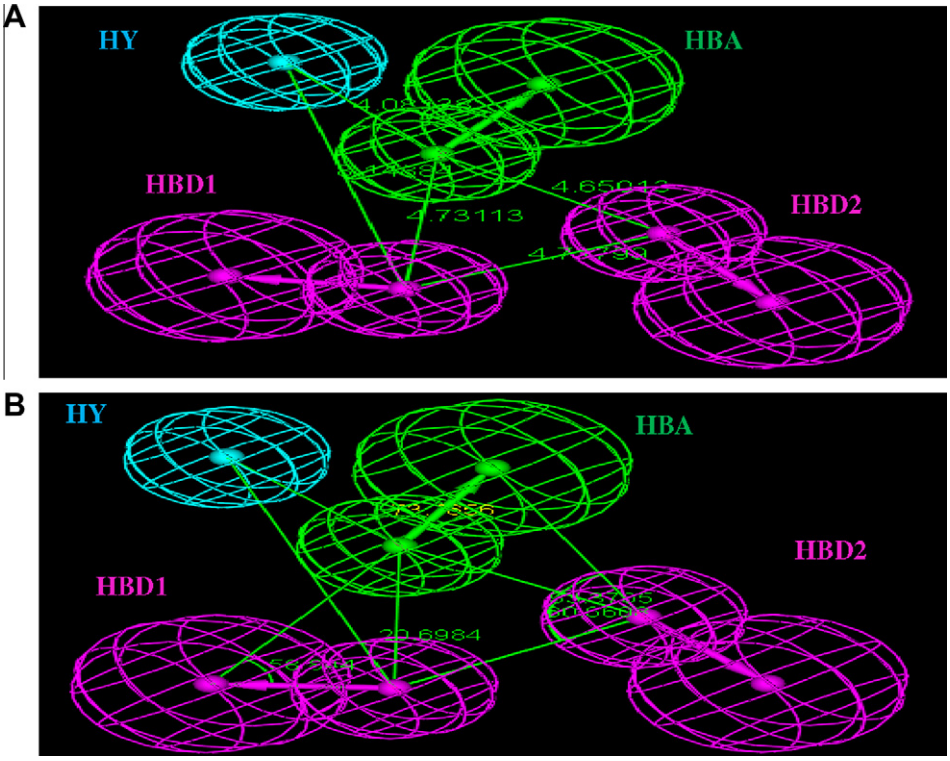

Figure 3. (A and B) Constraint distances and angles of CDK2 inhibitors hypothesis. The chemical features colored light blue, green and violet represent HY, HBA and HBD, respectively.

features namely; hydrogen bonding acceptor (HBA, green color), two hydrogen bonding donor (HBD1 and HBD2, violet color) and hydrophobic features (HY, blue color).

Previously, Vadivelan et al.[39] reported a ligand-based Pharmacophore model for CDK2 inhibitors that contains the same kind and number of features; two hydrogen bonding acceptor (HBA), one hydrogen bonding donor (HBD) and one hydrophobic feature (HY). Yet, the reported co-crystal structure of CDK2/ATP as well as the crystal structure of CDK2 with several inhibitors[40–43] disproved the latter model. These crystal structures revealed that the mode of binding in the CDK2/ATP binding pocket along the residues Glu81–Leu83 is represented as a donor–acceptor–donor motif. This binding mode is consistent with our generated pharmacophore which contains HBD1, HBA, and HBD2 in a similar manner.

In this article we reported the constraint distances and the angles between the essential features existed in the generated hypothesis, as shown in Figure 3 and Table 1.

The structures of the test set **10, 11, 13a,b, 15a–d, 16a–d** were built and prepared using the Discovery Studio software and their conformational models were generated in the energy range of 20 kcal/mol above the estimated global energy minima. The mapping was carried out using Best Fit algorithm, during the Compare/Fit process. Different mapping for all the conformers of each compound to the hypothesis were visualized and the fit values of the best-fitting conformers were recorded (Fig. 4, Table 2).

2.3.3. Molecular docking studies of CDK2 inhibitors and binding conformation

All dock runs were conducted using MOE software. The 3D structure of the enzyme was used to detail intermolecular interactions between the ligand and the target protein. An automated docking study was carried out using the crystal structure of inhibitor **5**/CDK2 complex; having resolution of 1.95 Å. The prepared protein was used in the determination of the important amino acids in the predicted binding pocket.[30] The performance of the docking method on CDK inhibitors was evaluated by re-docking crystal ligand with 0.00974 RMSD value.[44] The docking process was carried out for the test set compounds (**10, 11, 13a,b, 15a–d, 16a–d**) using the compound energy as a scoring function.

In the flexible-ligand-rigid enzyme docking, the enzyme was represented by potential energy maps, namely, electrostatic, hydrogen bond, hydrophobic, and van der Waals. Interactive docking was carried out for all the conformers of each compound of the test set to the selected active site of CDK2.

The predicted binding energies of the compounds are recorded in the Table 2. The docking of ligand **5** and highly active molecule **13a** into the active site of CDK2 was performed (Fig. 5).

The docking results suggested that; first, the *p*-tosyl group will increase the hydrophobic binding interaction with the deep hydrophobic pocket created by His 84, Phe 80, Glu81 and Ala 84. Second, the hydrogen bonding interactions have been found, between the crucial features of compounds with the high docking scores and N–H group of Lys33, N–H of Lys89 and Asp86. Moreover, replacement of the purine ring system by imidazolidinone or opening the heterocyclic ring will decrease the docking value.

Alignment study of docked compound **13a** and ligand **5** with the binding pocket of CDK2 protein (Fig. 5D) revealed that (i) purine ring system of compound **13a** was perfectly aligned with purine nucleus of ligand **5**, (ii) carboxamide side chain superimposed with *O*-pyrrolidin-2-one methyl substituent of ligand **5**, (iii) additionally, both the ligand **5** and compound **13a** make the same hydrogen bonding interaction with Asp86 and Lys33.

Each docked compound was assigned a score according to its fit in the LBP (Table 2).

2.3.4. Conclusion of molecular modeling

The above molecular docking study provides useful information for understanding the structural features of CDK2 inhibitors. The

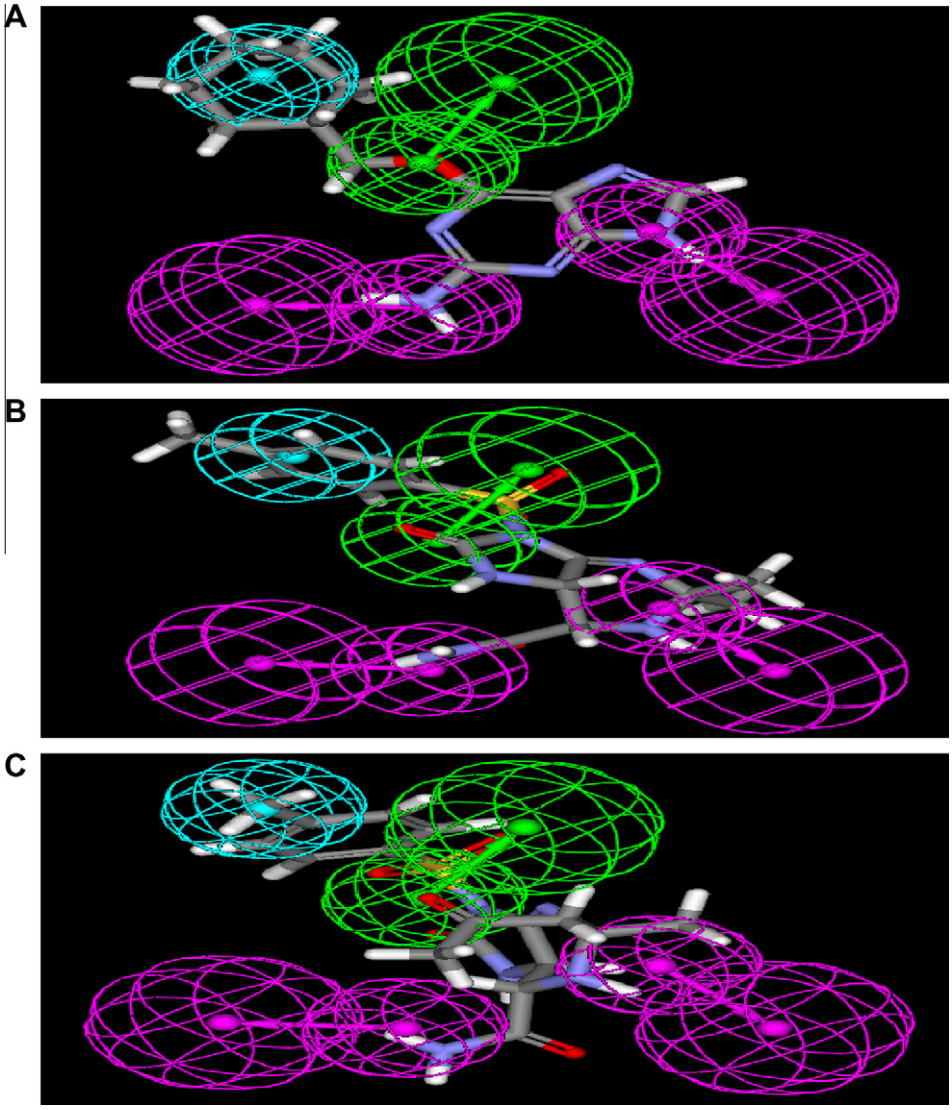

Figure 4. (a–c) Mapping of CDK2 inhibitors pharmacophore with lead compound **8** (NU2058) and compounds **13a** and **13b**, respectively.

Table 1
Constraint distances and angles between the features of generated CDK2 inhibitors hypothesis

Dimensions	Features of CDK2 inhibitors hypothesis
Constraint distances (Å) between features	HBD1–HBD2, 4.787; HBD1–HBA, 4.731; HBD2–HBA, 4.650; HBD1–HY, 8.488; HBA–HY, 4.081
Constraint angles (Å) between features	HBA–HBD1–HBD2, 30.698; HBD1–HBD2–HBA, 60.660; PI–HY2–HY3, 90.74; HBA–HBD1 vector, 58.814.; HBD2–HBA vector, 53.370

binding mode of the newly constructed CDK2 inhibitors pharmacophore model was compatible with that obtained from the reported crystal structures.[40–43] The most potent purine derivatives **13a,b** (IC_{50} values of 14 ± 9 and 13 ± 9 μM, respectively) showed the highest docking scores and fit values. This was extended to the successful designing of highly active analogs of purine derivatives against CDK2.

3. Structural activity relationship (SAR)

The structural activity relationship (SAR) of newly synthesized compounds **10, 11, 13a,b, 15a–d** and **16a–d**, explored the importance of the planer bicyclic purine system in cycline-dependent kinase2 CDK2/cyclin A3 inhibition activity and to certain extent in the in vitro antitumor activity. Among the test compounds a contrast biological relations are observed between a cyclic urea derivative **10** and cyclic purine derivatives **13a,b.** Presence of lipophilic function (LF) such as *para*-tosyl group in compounds (**10, 13a,b**) in addition 2-methyl and 2-(2-oxopropyl) moieties of cyclic purine derivatives **13a,b**; showed the highest cycline-dependent kinase2 (CDK2) inhibitory activity together with appreciated antitumor activity against EAC cells for **13a,b** and vice versa for compound **10**. Electron donating group (EDG) on *para* position of benzylidene moiety for Compounds **15a–d**; increase antitumor agent against EAC (**15a**). While the insertion of such group in other position provided lower potency (**15b–d**). 2,3-Dimethoxy substitution on benzylidene moiety of pyrimidine derivatives (**16d**) induced steric clash and revealed lower potency as shown in (Fig. 7).

Table 2
Best fit value and docking scour for each compound in the test set (**12**, **13**, **15a**,**b**, **17a**–**d**, **18a**–**d**) mapped with active site of CDK2

Compd No.	Docking value (kcal/mol)	Fit value
Ligand **5**	−12.01	3.89
10	−12.97	2.93
13a	−13.51	3.79
13b	−13.18	3.87
15a	−11.28	2.76
15b	−10.66	1.99
15c	−10.86	1.87
15d	−11.97	2.10
16a	−12.91	2.45
16b	−11.44	2.34
16c	−12.87	1.92
16d	−13.19	2.81
11	−10.67	2.66

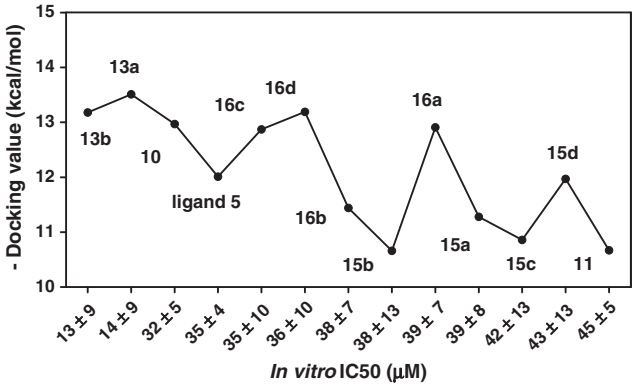

Figure 6. The in vitro IC_{50} of the test set compounds versus their docking scores against cycline-dependent kinase2 CDK2/cyclin A3 docking scores of ligand **5** and the newly synthesized compounds mapped with active site of cycline-dependent kinase2 (CDK2) are diagramed against their corresponding IC_{50}/μM in vitro CDK2 inhibitory activity. Except for pyrimidine derivatives **16a**–**d**, the in vitro CDK2 inhibitory activity of the designed compounds was found to approximately match with the docking values comparing to ligand **5**. As an example of pyrimidine derivatives, it was compound **16d** that did not exhibit significant in vitro activity against CDK2 (Table 3) in spite of having a better docking score value than the reference ligand **5**. This could be explained by a clash region predicted to exist between **16d** and some amino acid residues of CDK2 (Fig. 7). This clash region was constructed through the existence of some atoms of **16d** outside the binding pocket.

4. Experimental section

4.1. Chemistry

DAMN was obtained from Aldrich and used without further purification. The aromatic aldehydes were obtained from Merck. The reactions were carried out by mixing the reagents directly from the bottle with a solvent. Infrared spectra were recorded on a Perkin–Elmer Paragon FT-IR instrument. NMR spectra were recorded in DMSO-d_6 at room temperature on a Bruker AMX 400 Avance operating at 400 (1H) and 100 MHz (13C), respectively. Melting points were taken with an Electro-thermal Apparatus and are uncorrected.

4.1.1. *N*-{[(*Z*)-2-Amino-1,2-dicyanovinyl]amino}carbonyl]-4-methylbenzenesulfonamide (10)

A solution of DAMN (0.60 g, 5.55 mmol) in dry acetonitrile (10 mL) was kept stirring in an ice bath, under nitrogen atmosphere, in a round-bottom flask equipped with a serum cap, toluene sulfonyl-isocyanate (1 mL, 5.88 mmol) was added drop-wise with a syringe through the serum cap, and 10 min later a precipitate start to appear. The mixture was stirred at room temperature for 24 h, when the cream solid was filtered and washed with acetonitrile and diethyl ether, the product was identified as the title compound (1.60 g) of white powder. The product characterization was; Yield: 94%; mp >300 °C (from ethanol, lit.[3,11]: >300 °C); IR: (Nujol mull) 2255 (m, CN), 2209 (s, CN), 1645 (s, C=O), 1611

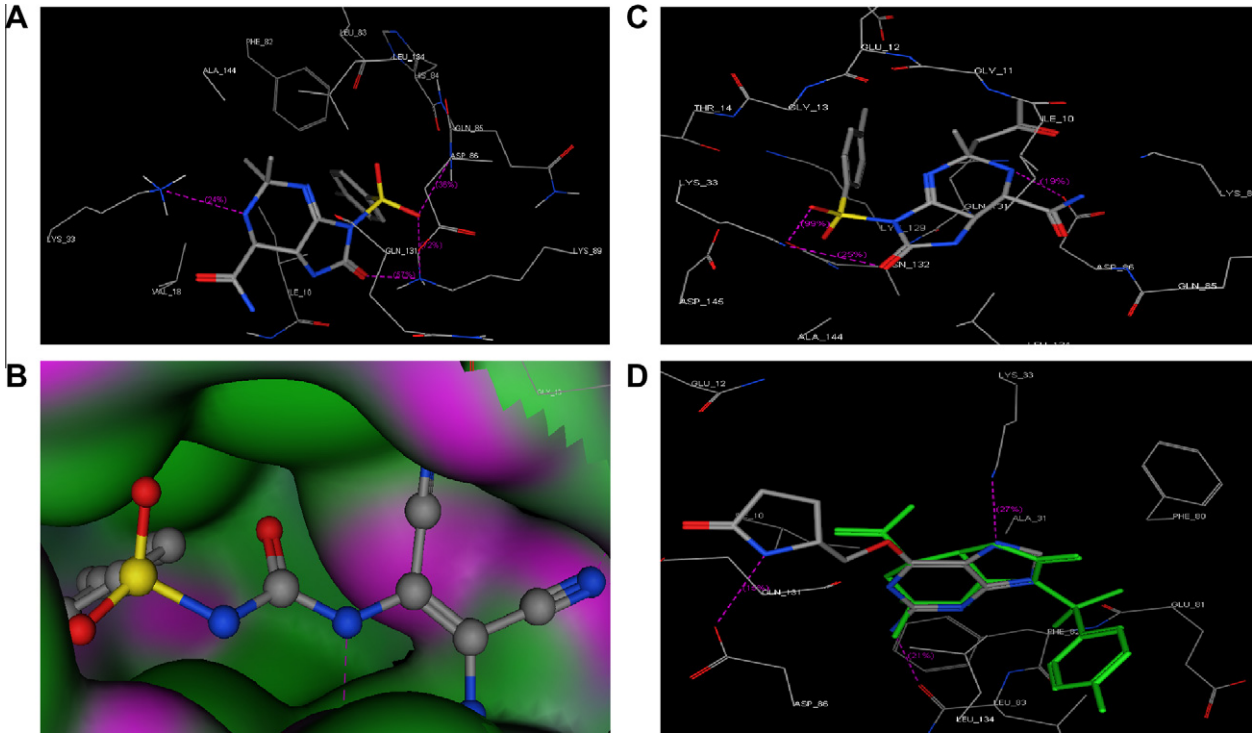

Figure 5. (A–C) The proposed binding mode of compounds **13a** (A), **13b** (C) and **10** (B) inside the active site of CDK2 resulting from docking, respectively. The most important amino acids are shown together with their respective numbers. Compound **13a** form four hydrogen bonds with tow Lys89 and two with Lys33 and Asp86. (D) Alignment of docked compound **13a** (green color) and ligand **5** with the binding pocket.

Table 3
CDK2 inhibition and the cytotoxic activity of the newly synthesized compounds on EAC cells

Compounds	Cell growth inhibition (GI_{50}/μM)	CDK2/cyclin A3 (IC_{50}/μM)
10	12 ± 8	32 ± 5
11	28 ± 6	45 ± 5
13a	15 ± 5	14 ± 9
13b	16 ± 5	13 ± 9
15a	10 ± 6	39 ± 8
15b	26 ± 6	38 ± 13
15c	25 ± 9	42 ± 13
15d	2 7 ± 6	43 ± 13
16a	17 ± 2	39 ± 7
16b	16 ± 1	38 ± 7
16c	19 ± 6	35 ± 10
16d	21 ± 6	36 ± 10
Ligand **5**[30]	18 ± 5	35 ± 4%

IC_{50} value; corresponds to the compound concentration causing 50% mortality in net cells.
IC_{50} >100 μg mL is considered inactive.[30] the biological value of ligand **5** as reported in lit.

(s, C═C); ^{1}H NMR: (DMSO-d_6, 300 MHz) δ 2,4 (s, 3H, CH3), 7.38 (s, 2H, NH_2), 7.41 (d, 2H, J = 7.9 Hz, Ar-H), 7.77 (s, 1H, –NHCO), 7.79 (d, 2H, J = 7.9 Hz, Ar-H), 11.18 (s, H, CONHTos); ^{13}C NMR: δ 106.1, 113.7, 117.0, 129.7, 149.8, 127.5, 129.5, 137.0, 144.0, 21.0. Anal. Calcd for $C_{12}H_{11}N_5O_3S$ (mol. wt. 305.3): C, 47.21; H, 3.63; N, 22.94; S, 10.50. Found: C, 47.12; H, 3.61; N, 22.89; S, 10.56.

4.1.2. 5-Cyano-*N*-[(4-methylphenyl)sulfonyl]-2-oxo-2,3-dihydro-1*H*-imidazole-4-carboximidamide (11)

To a suspension of compound **10** (0.35 g, 1.14 mmol) in acetonitrile (2 mL) under nitrogen atmosphere at 0 °C, DBU (43 mL, 0.043 g, 0.28 mmol) was added and then stirred at rt for 2 h. The solid product was collected by filtration and washed with acetonitrile to give compound **11** as a cream white solid. Recrystallization from ethanol gave colorless powder. Yield: 91% (0.32 g); mp 263–265 °C (from ethanol, lit.[7] 262–263 °C); IR: λ_{max}/cm^{-1}: 3285, 3070, 2236,1724, 1663, 1658; ^{1}H NMR: (DMSO-d_6, 300 MHz) δ 2,6 (s, 3H, CH_3), 7.36 (d, 2H, J = 8.7 Hz, CHTos), 7.78 (d, 2H, J = 8.7 Hz, CHTos), 8.41 (s, 1H, NH), 11.3 (s, 1H, NH), 11.7 (s, 1H, NH), 11.51 (s, H, CONHTos); ^{13}C NMR: δ 96.9, 110.8 (CN), 126.6 (CN), 150.9, 157.6 (C═N), 126.2, 129.3, 139.1, 142.7, 21.0. Anal. Calcd for $C_{12}H_{11}N_5O_3S$ (mol. wt. 305.3): C, 47.21; H, 3.63; N, 22.94; S, 10.50. Found: C, 47.23; H, 3.72; N, 22.82; S, 10.59. The spectral data were consistent with literature values.[7]

4.1.3. 2,2-Dimethyl-9-[(4-methylphenyl)sulfonyl]-8-oxo-2,7,8,9-tetrahydro-1*H*-purine-6-carboxamide (13a)

DBU (274 μL, 0.274 g, 2.20 mmol) was added to a suspension of diaminomaleonitrile urea (0.35 g, 1.14 mmol) in acetone (4 mL) at 0 °C, and the reaction mixture was stirred at room temperature in a flask equipped with a screem caps under nitrogen. A solid precipitate started to develop after 3 h, and the reaction mixture was stirred for another 24 h. The solid was filtered and washed with acetone and diethyl ether to give the title compound (0.15 g, 45% yield) as a cream yellow color. TLC (silica gel; ethanol/CH_2Cl_2; 1:9) R_f = 0.72. Characterization; mp 235–237 °C dec; IR (Nujol mull) 3446 (NH), 3289.8 (NH_2), 2970, 2955, 1679 (s, C═O); 1636.4 (s, C═O), 1567.6; ^{1}H NMR: (DMSO-d_6, 300 MHz) δ 1.61 (s, 6H, -C(CH3)$_2$), 2,42 (s, 3H, CH_3), 6.98 (s, 2H, NH_2), 7.40 (d, 2H, J = 7.8 Hz, CHTos), 7.92 (d, 2H, J = 8.1 Hz, CHTos), 9.71 (s, 1H, NH), 11.35 (s, 1H, NH); ^{13}C NMR: δ 21.3, 27.5, 69.0, 114.6, 126.9, 127.2, 129.9, 140.7, 143.5, 148.67, 151.1, 160.3. Anal. Calcd for $C_{15}H_{17}N_5O_4S$ (mol. wt. 363.39): C, 49.58; H, 4.72; N, 19.27; S, 8.82. Found: C, 49.52; H, 5.15; N, 19.30; S, 8.39.

4.1.4. 2-Methyl-9-[(4-methylphenyl)sulfonyl]-8-oxo-2-(2-oxopropyl)-2,7,8,9-tetrahydro-1*H*-purine-6-carboxamide (13b)

DBU (274 μL, 0.274 g, 2.20 mmol) was added to a suspension of diaminomaleonitrile urea (0.70 g, 2.28 mmol) in acetyl acetone (205.6 μL, 2 mmol) at 0 °C, and the reaction mixture was stirred at room temperature in a flask equipped with a screem cap under nitrogen. A solid precipitate started to develop after 3 h, and the reaction mixture was stirred for another 24 h. The solid was filtered and washed with acetone to give the title compound (0.28 g, 46% yield) as pinkish color. TLC (silica gel; EtOH/CH_2Cl_2 1:9) R_f = 0.72. Characterization; mp 330–232 °C dec; IR (Nujol mull) 3450 (NH), 3290 (NH_2), 1735 (s, C═O); 1670 (s, C═O); 1640 (s, C═O); ^{1}H NMR: (DMSO-d_6, 300 MHz) δ 1.64 (s, 3H, –C–CH_3), 2.21 (s, 2H, –CH_2–), 2,42 (s, 3H, CH_3), 6.98 (s, 2H, NH_2), 7.36 (d, 2H, J = 7.8 Hz, CHTos), 7.86 (d, 2H, J = 7.8 Hz, CHTos), 9.70 (s, 1H, NH), 11.32 (s, 1H, NH); ^{13}C NMR: δ 21.3, 24.5, 27.5, 67.8, 69.0, 114.6, 126.9, 127.2, 129.9, 140.7, 143.5, 148.67, 151.1, 160.3, 206.3. Anal. Calcd for $C_{17}H_{19}N_5O_5S$ (mol. wt. 405.43): C, 50.36; H, 4.72; N, 17.27; S, 7.91. Found: C, 50.49; H, 4.92; N, 17.85; S, 8.13.

4.1.5. General procedure for the synthesis of 1-(tosyl-3-[2-(-(2,3,4,5,6-pentasubsituttedbenzylidene-amino)-1,2-dicycano-vinyl]-urea (15a–d) and *N*-[5-(2,3,4,5,6-pentasubstitutedphenylmethylene-amino)-6-cyano-2-oxo-2,3-dihydro-pyrimidin-4-yl]-4-methyl-benzenesulfonamide (16a–d)

Under vigorous stirring a mixture of diaminomaleonitrile DAMN-urea (2 mmol) and the respective corresponding aldehydes **14a–d** (4 mmol) were suspended in ethanol (5 mL) and triethylamine (4 mmol) was slowly added at 0 °C for 10 min and stirring the reaction mixture was continued for 2–3 h at room temperature until the color changed from yellow to white then to red after 5 h. which were allowed to stand overnight until a precipitate appeared. The solid was filtered off, washed with ethanol and dried under reduced pressure and recrystallized from methanol to produce the first portion **15a–d** whereupon the reaction mixtures solidified in good yields. The A homogeneous solution of mother liquor was continued stirring for 24 h until the second portion of crude products obtained which was filtered off and washed with ethanol and recrystallized from methanol. The products, unless otherwise noted, were yellow solids of **16a–d**.

4.1.6. *N*-{[((*Z*)-1,2-Dicyano-2-{[(1*E*)-(4-methoxyphenyl)methylene]amino}vinyl) amino]carbonyl}-4-methylbenzenesulfonamide (15a)

Reddish solid, yield: (0.60 g, 70%); mp >300 °C dec (from methanol); IR (Nujol mull) 3353 (s, NH), 3259 (s, NH), 2955, 2854, 2205 (CN), 1919.3 (CN), 1655 (s, C═O); 1600 (s, C═O); 1527 (s, C═O), 1461; ^{1}H NMR: (DMSO-d_6, 300 MHz) δ 2.35 (s, 3H, CH3), 3.85 (s, 3H, OCH_3), 7.13 (d, 2H, J = 8.7 Hz, CHAr), 7.25 (s, 1H, –N═CH), 7.36 (d, 2H, J = 8.4 Hz, CHTos), 7.71 (d, 2H, J = 8.1 Hz, CHTos), 7.87 (d, 2H, J = 8.7 Hz, CHAr), 9.10 (s, 1H, NH), 9.86 (s, 1H, NH); ^{13}C NMR (DMSO-d_6, 750 MHz): δ 21.0, 55.6, 98.0, 110.8, 114.5, 126.2, 126.5, 126.6, 128.0, 129.3, 129.5, 132.3, 139.1, 142.7, 150.9, 151.6, 163.1. Anal. Calcd for $C_{20}H_{17}N_5O_4S$: C, 56.73; H, 4.05; N, 16.54, S, 7.57. Found: C, 56.87; H, 4.19; N, 16.43; S, 7.90.

4.1.7. *N*-{[((*Z*)-1,2-Dicyano-2-{[(1*E*)-(2,4,6-trimethoxyphenyl)-methylene]amino}vinyl) amino]carbonyl}-4-methylbenzenesulfonamide (15b)

Yield: (0.75 g, 77%); mp >300 °C dec (from methanol); IR (Nujol mull) 3530 (s, NH), 3279.8 (br s, NH), 2922, 2844, 2235.9 (CN), 1720 (s, C═O); 1663.9 (s, C═O); 1620.2, 1556.8 (s, C═O); ^{1}H NMR: (DMSO-d_6, 300 MHz) δ 2.34 (s, 3H, CH_3), 3.85 (s, 3H, OCH_3), 3.81 (s, 6H, 2OCH_3), 7.12 (d, 2H, J = 8.7 Hz, CHAr), 7.26 (s, 1H, –N═CH), 7.36 (d, 2H, J = 8.4 Hz, CHTos), 7.79 (d, 2H, J = 8.4 Hz, CHTos), 7.87 (d, 2H, J = 8.7 Hz, CHAr), 8.37 (s, NH), 8.40

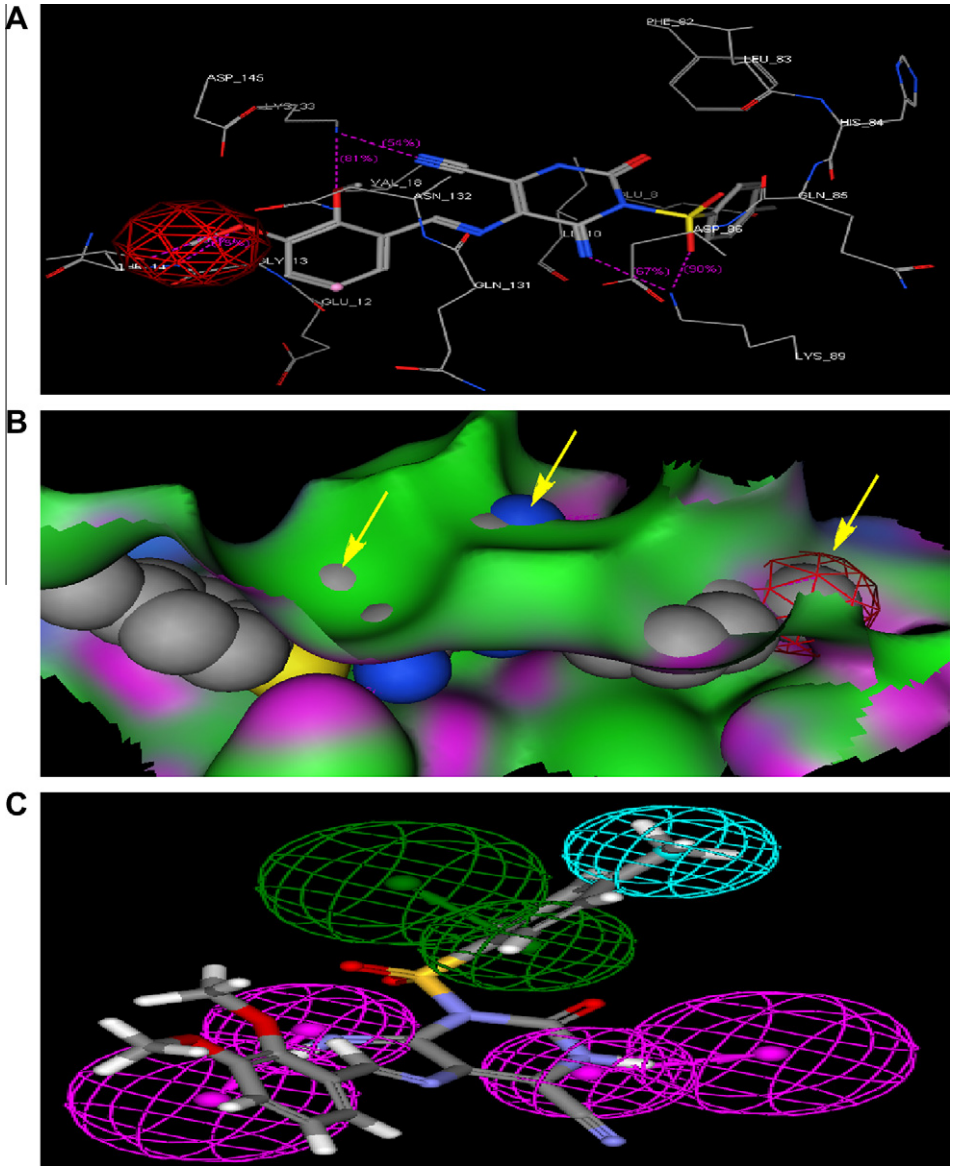

Figure 7. (A and B) Docking of compound **16d** to the active site of CDK2 shows its hydrogen bond interactions and its clash with binding site (C) Mapping of CDK2 inhibitors pharmacophore with **16d**, with non optimum fitting interaction.

(s, 2H, CHAr), 11.50 (br s, NH); ^{13}C NMR (DMSO-d_6, 750 MHz): δ 21.2, 55.5, 55.6, 105, 112.9, 114.8, 126.9, 128.5, 129.9, 130.3, 132.3, 139.1, 141.4, 151.1, 153.2, 165.5, 167.1. Anal. Calcd for $C_{22}H_{21}N_5O_6S$ (mol. wt. 483.5): C, 54.65; H, 4.38; N, 14.48, S, 6.63. Found: C, 54.47; H, 4.23; N, 14.33; S, 6.55.

4.1.8. *N*-{[((*Z*)-1,2-Dicyano-2-{[(1*E*)-(3,5-dimethoxyphenyl)-methylene]amino}vinyl) amino]carbonyl}-4-methylbenzene-sulfonamide (15c)

Pink solid, yield: (0.86 g, 94%); mp >300 °C dec (from methanol); IR (Nujol mull) 3280 (br s, NH), 2236 (CN), 1720 (s, C=O); 1664, 1557; ^{1}H NMR: (DMSO-d_6, 300 MHz) δ 2.34 (s, 3H, CH_3), 3.84 (s, 6H, 2OCH_3), 7.15 (d, 2H, J = 8.7 Hz, CHAr), 7.27 (s, 1H, –N=CH), 7.35 (d, 2H, J = 8.4 Hz, CHTos), 7.73 (s, 1H, CHAr), 7.80 (d, 2H, J = 8.4 Hz, CHTos), 7.88 (d, 2H, J = 8.7 Hz, CHAr), 78.37 (s, NH), 8.40 (s, 2H, CHAr), 11.50 (br s, NH); ^{13}C NMR (DMSO-d_6, 750 MHz): δ 21.2, 55.5, 106, 113.1, 114.5, 127.1, 128.3, 129.7, 130.6, 132.5, 139.5, 141.6, 151.5, 153.9, 164.5, 166.1. Anal. Calcd for $C_{21}H_{19}N_5O_5S$ (mol. wt. 453.47): C, 55.62; H, 4.22; N, 15.44, S, 7.07. Found: C, 55.68; H, 4.32; N, 15.42; S, 7.05.

4.1.9. *N*-{[((*Z*)-1,2-Dicyano-2-{[(1*E*)-(2,3-dimethoxyphenyl)-methylene]amino}vinyl) amino]carbonyl}-4-methylbenzene-sulfonamide (15d)

Yield: (0.78 g, 86%); mp >300 °C dec (from methanol); IR (Nujol mull) 3285 (br s, NH), 2233 (CN), 1723 (s, C=O); 1665, 1559; ^{1}H NMR: (DMSO-d_6, 300 MHz) δ 2.35 (s, 3H, CH_3), 3.85 (s, 6H, 2OCH_3), 7.13 (d, 1H, J = 8.7 Hz, CHAr), 7.25 (s, 1H, –N=CH), 7.35 (d, 2H, J = 8.4 Hz, CHTos), 7.73 (d, 1H, J = 8.7 Hz, CHAr), 7.80 (d, 2H, J = 8.4 Hz, CHTos), 7.88 (dd, 1H, J = 2.8, 8.7 Hz, CHAr), 78.37 (s, NH), 8.40 (s, 2H, CHAr), 11.50 (br s, NH); ^{13}C NMR (DMSO-d_6, 750 MHz): δ 21.2, 55.5, 106, 113.1, 114.5, 127.1, 128.3, 129.7, 130.6, 132.5, 139.5, 141.6, 151.5, 153.9, 164.5, 166.1. Anal. Calcd for $C_{21}H_{19}N_5O_5S$ (mol. wt. 453.47): C, 55.62; H, 4.22; N, 15.44, S, 7.07. Found: C, 55.38; H, 4.26; N, 15.24; S, 6.98.

4.1.10. 6-Amino-5-{[(1*E*)-(4-methoxyphenyl)methylene]-amino}-1-[(4-methylphenyl)sulfonyl]-2-oxo-1,2-dihydro-pyrimidine-4-carbonitrile (16a)

Reddish solid re-crystallization from acetonitrile, yield: (0.55 g, 65%); mp >300 °C dec (from methanol); IR (Nujol mull) 3355–3260

(br s, NH_2), 2230 (CN), 1655 (s, C=O); 1610, 1550, 1461; ^{1}H NMR: (DMSO-d_6, 300 MHz) δ 2.35 (s, 3H, CH3), 3.84 (s, 3H, OCH_3), 7.12 (d, 2H, J = 8.7 Hz, CHAr), 7.26 (s, 1H, –N=CH), 7.36 (d, 2H, J = 8.4 Hz, CHTos), 7.72 (d, 2H, J = 8.1 Hz, CHTos), 7.88 (d, 2H, J = 8.7 Hz, CHAr), 9.10–9.86 (br s, 2H, NH2); ^{13}C NMR (DMSO-d_6, 750 MHz): δ 21.5, 55.8, 97.9, 110.5, 114.2, 126.3, 126.6, 126.7, 128.1, 129.5, 129.8, 132.2, 139.4, 142.1, 151.3, 151.9, 163.7. Anal. Calcd for $C_{20}H_{17}N_5O_4S$: C, 56.73; H, 4.05; N, 16.54, S, 7.57. Found: C, 56.87; H, 4.19; N, 16.43; S, 7.90.

4.1.11. 6-Amino-5-{[(1*E*)-(2,4,6-trimethoxyphenyl)methylene]-amino}-1-[(4-methylphenyl) sulfonyl]-2-oxo-1,2-dihydropyrimidine-4-carbonitrile (16b)

Yield: (0.65 g, 67%); mp >300 °C dec (from methanol); IR (Nujol mull) 3335–3280 (br s, NH_2), 2235 (CN), 1664 (s, C=O); 1620.2, 1557; ^{1}H NMR: (DMSO-d_6, 300 MHz) δ 2.35 (s, 3H, CH_3), 3.85 (s, 3H, OCH_3), 3.82 (s, 6H, $2OCH_3$), 7.15 (d, 2H, J = 8.7 Hz, CHAr), 7.25 (s, 1H, –N=CH), 7.36 (d, 2H, J = 8.4 Hz, CHTos), 7.80 (d, 2H, J = 8.4 Hz, CHTos), 7.89 (d, 2H, J = 8.7 Hz, CHAr), 8.37 (s, NH_2), 8.40 (s, 2H, CHAr); ^{13}C NMR (DMSO-d_6, 750 MHz): δ 21.0, 55.3, 55.5, 104, 112.1, 114.4, 126.5, 128.6, 129.4, 130.6, 132.8, 139.6, 141.5, 151.8, 153.9, 163.7, 166.3. Anal. Calcd for $C_{22}H_{21}N_5O_6S$ (mol. wt. 483.5): C, 54.65; H, 4.38; N, 14.48, S, 6.63. Found: C, 54.55; H, 4.16; N, 14.23; S, 6.46.

4.1.12. 6-Amino-5-{[(1*E*)-(3,5-dimethoxyphenyl)methylene]-amino}-1-[(4-methylphenyl) sulfonyl]-2-oxo-1,2-dihydropyrimidine-4-carbonitrile (16c)

Yield: (0.66 g, 72%); mp >300 °C dec (from methanol); IR (Nujol mull) 3280 (br s, NH_2), 2236 (CN), 1665 (s, C=O), 1557; ^{1}H NMR: (DMSO-d_6, 300 MHz) δ 2.35 (s, 3H, CH_3), 3.83 (s, 6H, $2OCH_3$), 7.15 (d, 2H, J = 8.7 Hz, CHAr), 7.26 (s, 1H, –N=CH), 7.36 (d, 2H, J = 8.4 Hz, CHTos), 7.77 (s, 1H, CHAr), 7.81 (d, 2H, J = 8.4 Hz, CHTos), 7.87 (d, 2H, J = 8.7 Hz, CHAr), 78.37 (s, NH_2), 8.41 (s, 2H, CHAr); ^{13}C NMR (DMSO-d_6, 750 MHz): δ 21.2, 55.5, 105, 112.1, 114.2, 126.8, 128.1, 129.4, 130.2, 132.8, 139.35, 141.2, 151.7, 153.5, 163.9, 164.6. Anal. Calcd for $C_{21}H_{19}N_5O_5S$ (mol. wt. 453.47): C, 55.62; H, 4.22; N, 15.44, S, 7.07. Found: C, 55.68; H, 4.32; N, 15.42; S, 7.05.

4.1.13. 6-Amino-5-{[(1*E*)-(2,3-dimethoxyphenyl)methylene]-amino}-1-[(4-methylphenyl) sulfonyl]-2-oxo-1,2-dihydropyrimidine-4-carbonitrile (16d)

Yield: (0.58 g, 63%); mp >300 °C dec (from methanol); IR (Nujol mull) 3285 (br s, NH_2), 2230 (CN), 1665 (s, C=O), 1559; ^{1}H NMR: (DMSO-d_6, 300 MHz) δ 2.34 (s, 3H, CH_3), 3.84 (s, 3H, OCH_3), 3.81 (s, 3H, OCH_3), 7.12 (d, 1H, J = 8.7 Hz, CHAr), 7.26 (s, 1H, –N=CH), 7.36 (d, 2H, J = 8.4 Hz, CHTos), 7.74 (d, 1H, J = 8.7 Hz, CHAr), 7.81 (d, 2H, J = 8.4 Hz, CHTos), 7.87 (dd, 1H, J = 2.8, 8.7 Hz, CHAr), 78.37 (s, NH_2); ^{13}C NMR (DMSO-d_6, 750 MHz): δ 21.1, 55.3, 105.6, 112.1, 114.2, 126.1, 128.5, 129.3, 130.9, 132.3, 139.6, 141.4, 151.3, 153.7, 163.9, 165.3. Anal. Calcd for $C_{21}H_{19}N_5O_5S$ (mol. wt. 453.47): C, 55.62; H, 4.22; N, 15.44, S, 7.07. Found: C, 55.68; H, 4.23; N, 15.40; S, 7.04.

4.2. Biological assays

4.2.1. CDK2/cyclin A3 inhibition assay

Inhibition of CDK2/cyclin A3 was assayed as previously described[45] using enzyme prepared from starfish oocytes (Marthasterias glacials) and an assay buffer comprised of 50 mM Tris–HCl 7.5, containing 5 mM $MgCl_2$. Cycline-dependent kinase2 CDK2/cyclin A3 was prepared as previously described[46] (cyclin A3 is a C-terminal cyclin A fragment encoding residues 171–432). The final ATP concentration in (CDK2) assay was 12.5 μM. The inhibitory activity for the test compound was explored as the measurement of IC_{50}/μM (Table 3), which is the concentration required inhibiting the enzyme activity by 50% under the assay conditions used.

4.2.1.1. Experimental procedure. Ninety-six-well high-binding microtiter ELISA plates were coated overnight at 4 °C with mouse anti-GST in PBS. The plates were decanted and blocked with ELISA buffer (0.05% bovine g-globulins [BGG] in 50 mM Tris-buffered saline [pH7.5] with 0.05% Tween 20 and 0.1 mM sodium *ortho* vanadate). The cyclin-dependent kinase reaction was performed in 96-well non-binding microtiter plates. ATP, CDK2/cyclinA3 (HIS tagged and phosphor T160), and GST-Rb were diluted in kinase reaction buffer (25 mM Tris-buffered saline [pH7.5] with 10 mM $MgCl_2$, 5 mM β-glycerophosphate, 2 mM DTT, 0.1 mM sodium *ortho* vanadate, and 0.005% Nonidet P-40). Final concentrations of ATP and CDK2 were 200 mM and 300 ppm, respectively. Compounds were diluted in 10% DMSO in kinase reaction buffer. ATP was added to each well of the kinase reaction plate, followed in sequence by GST-Rb and test compound serial dilutions. The cycline-dependent kinase reaction was started with the addition of CDK2/cyclin A3 to the kinase reaction plate and stopped with kinase stop buffer (50 mM EDTA in ELISA buffer). The ELISA plates were washed with ELISA wash buffer (50 mM Tris-buffered saline [pH 7.5] with 0.05% Tween 20 and 1 mM $MnCl_2$). The reactions were diluted 1:10 into kinase stop buffer in the ELISA plate. Phosphorylated Rb was detected with rabbit anti-phospho-Rb (Ser795) followed by (HRP)-linked IgG anti-rabbit antibody. The plate was developed with tetra-methyl benzylidene as substrate and the absorbance was measured at 450 nm.

4.2.2. In vitro antitumor assay

All chemicals and reagents are supplied from Sigma–Aldrich (SIGMA–ALDRICH Chemie GmbH, Steinheim, Germany). Animal house and biochemical equipments have been made available by the University of Karachi, Pakistan. Female Swiss albino mice weighing 25–30 g were used in this study (The Holding Company for Biological Products and Vaccines Karachi, Pakistan. Mice were housed at a constant temperature (24 ± 2 °C) with alternating 12 h-light and dark cycles and fed standard laboratory food and water. Tests were made in consideration of the internationally valid guidelines. The Medical Centre for Research, Karachi, Pakistan is concerned with biological and animal studies which have an approval of an institution responsible for animal ethics.

4.2.2.1. Cell growth inhibition assay. The in-vitro growth inhibitory activity of the test compounds against EAC cell line was evaluated in NCI. The evaluation depends on using the standard 48 h exposure assay. Determination of GI_{50}/μM of the test compounds was performed by preparation of serial dilutions ranged from 10^{-9} to 10^{-4} M[47] in a mixture of dimethyl-sulfoxide (DMSO)/saline. Relationships between the profile of cell growth inhibition produced by the test compounds and that of the established CDK inhibitor ligand **5**, was investigated using the COMPARE algorithm study.[48] Ehrlich ascites carcinoma (EAC) cells were obtained by needle aspiration of ascetic fluid from the pre-inoculated mice under aseptic conditions. Tumor cells suspension (2.5×10^6 per mL) was prepared in saline. The parent line was kindly supplied by the Dow Medical College (DMC), Diagnostics Lab., Karachi University, Pakistan. The tumor cells were maintained by weekly intra-peritoneal transplantation of cells.

4.3. Molecular modeling

4.3.1. Generation of CDK2 inhibitor hypothesis

The training set was selected as described above (Fig. 1). The generation of the pharmacophore model for CDK2 inhibitors was accomplished using Discovery Studio 2.5 software (Accelrys Inc.,

San Diego, CA, USA). Molecules were built and conformational models for each compound were generated automatically using the Prepare Ligands protocol. The prepared training set molecules were used for generation 3D pharmacophore using common features hypothesis generation protocol (Hip-Hop module). In this study, hydrogen bonding acceptor, two hydrogen bonding donor and hydrophobic region, were used as the chemical features, which were reported to be crucial for the CDK2 inhibitors activity. By this process we specified the crucial features required for binding with the CDK2 enzyme.

4.3.2. Molecular docking studies of CDK2 inhibitors

Docking Study was performed using the MOE software. Downloading the crystal structure of CDK2 enzyme complexes with inhibitor **5** was carried out from protein data bank website (PDB) entry 1H0V.[30] Regularization and optimization for protein and ligand were performed. Determination of the essential amino acids in binding site was carried out and compared with that present in literature. The performance of the docking method was evaluated by re-docking crystal ligand into the assigned active site of CDK2 to determine RMSD value. Interactive docking using was carried out for all the conformers of each compound of the test set (**10**, **11**, **13a**,**b**, **15a**–**d**, **16a**–**d**) to the selected active site. Each docked compound was assigned a score according to its fit in the ligand binding pocket (LBP) and its binding mod.

5. Conclusion

In conclusion, the manuscript describes the investigation of a series of novel purine, urea, imidazole and pyrimidine derivatives, which were prepared in good yield by using diaminomaleonitrile and tosylisocyanate in acetonitrile. Molecular modeling studies, including fitting to a 3D-pharmacophore model their docking into cyclin-dependent kinase2 (CDK2) active site were performed to understand the structural features of CDK2 inhibitors. Biological evaluation for both in vitro CDK2/cyclin A3 inhibition activity and antitumor activity in Ehrlich ascites carcinoma (EAC) cell based assay were also carried out. The most potent novel purine derivatives were found to show the highest docking scores and fit values, which appeared coherent with the obtained biological data.

Acknowledgements

The authors gratefully acknowledge Professor Soomro, Dow Medical College (DMC), Diagnostics Lab., Karachi University for the evaluation the antitumor activity for the newly synthesized compounds.

References and notes

1. Al-Azmi, A.; Elassar, A. Z. A.; Booth, B. L. *Tetrahedron* **2003**, *59*, 2749.
2. Alves, M. J.; Booth, B. L.; Proença, M. F. *J. Chem. Soc., Perkin Trans. 2* **1990**, 1705.
3. Booth, B. L.; Dias, A. M.; Proença, M. F.; Zaki, M. E. A. *J. Org. Chem.* **2001**, *66*, 8436.
4. Ohtsuka, Y. *J. Org. Chem.* **1978**, *43*, 3231.
5. Ohtsuka, Y. *J. Org. Chem.* **1979**, *44*, 827.
6. Erian, A. W. *Chem. Rev.* **1993**, *93*, 1991.
7. Hamad, A. S.; Derbala, H. A. Y. *J. Heterocycl. Chem.* **2001**, *38*, 939.
8. Rosemeyer, H. *Chem. Biodiv.* **2004**, *1*, 361; Bartoccini, F.; Cabri, W.; Celona, D.; Minetti, P.; Piersanti, G.; Tarzia, G. *J. Org. Chem.* **2010**, *75*, 5398.
9. Rida, S. M.; Ashour, F. A.; El-Hawash, S. A. M.; El-Semary, M. M.; Badr, M. H. *Arch. Pharm.* **2007**, *340*, 185.
10. Trova, M. P.; Schenectady, N.Y., US Patent 6969720–B2, 2005.
11. Pines, J. *Adv. Cancer Res.* **1995**, *66*, 181.
12. Sielecki, T. M.; Boylan, J. F.; Benfield, P. A.; Trainor, G. L. *J. Med. Chem.* **2000**, *43*, 1.
13. Arris, C. E.; Boyle, F. T.; Calvert, A. H.; Nicola, J. C.; Endicott, J. A.; Garman, A. F.; Gibson, A. E.; Golding, B. T.; Grant, S.; Griffin, R. J.; Jewsbury, P.; Johnson, L. N.; Lawrie, A. M.; Newell, D. R.; Noble, M. E. N.; Schultz, R.; Wu, Y. *J. Med. Chem.* **2000**, *43*, 2797.
14. Richardson, C. M.; Williamson, D. S.; Parratt, M. J.; Borgognoni, J.; Cansfield, A. D.; Dokurno, P.; Francis, J. L.; Howes, R.; Moor, J. D.; Murray, J. B.; Robertson, A.; Surgenor, A. E.; Torrance, C. J. *Bioorg. Med. Chem. Lett.* **2006**, *16*, 1353.
15. Harper, J. W.; Adams, P. D. *Chem. Rev.* **2001**, *101*, 2511.
16. Luk, K. C.; Simcox, M. E.; Schutt, A.; Rowan, K.; Thompson, T.; Chen, Y.; Kammlott, U.; DePinto, W.; Dunten, P.; Dermatakis, A. *Bioorg. Med. Chem. Lett.* **2004**, *14*, 913.
17. Castanedo, G.; Clark, K.; Wang, S.; Tsui, V.; Wong, M.; Nicholas, J.; Wickramasinghe, D.; Marsters, J. C.; Sutherlina, D. *Bioorg. Med. Chem. Lett.* **2006**, *16*, 1716.
18. Tang, J.; Shewchuk, L. M.; Sato, H.; Hasegawa, M.; Washio, Y.; Nishigaki, N. *Bioorg. Med. Chem. Lett.* **2003**, *13*, 2985.
19. Senderowicz, A. M.; Headlee, D.; Stinson, S. F.; Lush, R. M.; Kalil, N.; Villalba, L.; Hill, K.; Steinberg, S. M.; Figg, W. D.; Tompkins, A.; Arbuck, S. G.; Sausville, E. A. *J. Clin. Oncol.* **1998**, *16*, 2986.
20. Massagué, J. *Nature* **2004**, *432*, 298.
21. Grana, X.; Reddy, E. P. *Oncogene* **1995**, *11*, 211.
22. Morgan, D. O. *Nature* **1995**, *374*, 131.
23. Dynlacht, B. *Transcrip. Factors* **2001**, 85.
24. Pevarello, P.; Villa, M. *Expert Opin. Therapeutic Patents* **2005**, *15*, 675–703.
25. Shapiro, G. I. *J. Clin. Oncol.* **2006**, *24*, 1770.
26. Malumbres, M.; Barbacid, M. *Nat. Rev. Cancer* **2009**, *9*, 153.
27. Zaharevitz, D.; Kunick, C.; Schultz, C.; Meijer, L.; Leost, M.; Gussio, R.; Senderowicz, A.; Lahusen, T.; Sausville, E. *Am. Assoc. Cancer Res.* **1999**, 10. Philadelphia, PA.
28. Shewchuk, L.; Hassell, A.; Wisely, B.; Rocque, W.; Holmes, W.; Veal, J.; Kuyper, L. F. *J. Med. Chem* **2000**, *43*, 133.
29. Davies, T. J.; Bentley, J.; Arris, C. E.; Boyle, F. T.; Curtin, N. J.; Endicott, J. A.; Gibson, A. E.; Golding, B. T.; Griffin, R. J.; Hard castle, I. R.; Jews bury, P.; Johnson, L. N.; Mesguiche, V.; Newell, D. R.; Noble, M. E. M.; Tucker, J. A.; Wang, L.; Whitfield, H. J. *Nat. Struct. Biol.* **2002**, *9*, 745.
30. Gibson, A. E.; Arris, C. E.; Bentley, J.; Boyle, F. T.; Curtin, N. J.; Davies, T. G.; Endicott, J. A.; Golding, B. T.; Grant, S.; Griffin, R. J.; Jews bury, P.; Johnson, L. N.; Mesguiche, V.; Newell, D. R.; Noble, M. E. M.; Tucker, J. A.; Whitfield, H. J. *J. Med. Chem.* **2002**, *45*, 3381.
31. Dolle, R. E.; Le Bourdonnec, B.; Goodman, A. J.; Morales, G. A.; Salvino, J. M.; Zhang, W. *J. Comb. Chem.* **2007**, *9*, 855.
32. Schaumann, E.; Grabley, S. *Chem. Ber.* **1980**, *113*, 934.
33. Ohtsuka, Y. *J. Org. Chem.* **1976**, *41*, 629.
34. Wermuth, C. G. *Pharmacophore and Pharmacophore Searches*; Wiley-VCH, 2006. pp 3–13.
35. Ekins, S.; Mestres, J.; Testa, B. *J. Pharmacol.* **2007**, *152*, 9.
36. Ekins, S.; Mestres, J.; Testa, B. *J. Pharmacol.* **2007**, *152*, 21.
37. Raimundo, J. M.; Sudo, R. T.; Pontes, L. B.; Antunes, F.; Trachez, M. M.; Zapata-Sudo, G. *Eur. J. Pharmacol.* **2006**, *530*, 117.
38. Ismail, N. S. M.; Salah El Dine, R.; Hattori, M.; Takahashi, K.; Ihara, M. *Bioorg. Med. Chem.* **2008**, *16*, 7877.
39. Vadivelan, S.; Sinha, B. N.; Irudayam, S. J.; Jagarlapudi, S. A. R. P. *J. Chem. Inf. Model.* **2007**, *47*, 1526.
40. Schulze-Gahmen, U.; De Bondt, H.; Kim, S.-H. *J. Med. Chem.* **1996**, *39*, 4540.
41. Hoessel, R.; Leclerc, S.; Endicott, J. A.; Nobel, M. E. M.; Lawrie, A.; Tunnah, P.; Leost, M.; Damiens, E.; Marie, D.; Marko, D.; Niederberger, E.; Tang, W.; Eisenbrand, G.; Meijer, L. *Nat. Cell Biol.* **1999**, *1*, 60.
42. Bramson, N. H.; Corona, J.; Davis, S. T.; Dickerson, S. H.; Edelstein, M.; Frye, S. V.; Gampe, R. T.; Harris, P. A.; Hassel, A.; Holmes, W. D.; Hunter, R. N.; Lackey, K. E.; Lovejoy, B.; Luzzio, M. J.; Montana, V.; Rocque, W. J.; Rusnak, D.; Shewchuck, L.; Veal, J. M.; Walker, D. H.; Kuyper, L. F. *J. Med. Chem.* **2001**, *44*, 4339.
43. Huang, P.; Ramphal, J.; Rice, A.; Tang, F.; Liang, C.; Wei, J.; McMahon, G.; Tang, C. *Proc. Am. Assoc. Cancer Res.* **2001**, 42. Abst. 3622.
44. Abd El-Salam, O. I.; Abou El Ella, D. A.; Ismail, N. S. M.; Abdullah, M. *Pharmazie* **2009**, *64*, 147.
45. Vesely, J.; Havlicek, L.; Strnad, M.; Blow, J. J.; Donella-Deana, A.; Pinna, L.; Letham, D. S.; Kato, J.-Y.; Detivaud, L.; Leclerc, S.; Meijer, L. *Eur. J. Biochem.* **1994**, *224*, 771.
46. Brown, N. R.; Noble, M. E. M.; Lawrie, A. M.; Morris, M. C.; Tunnah, P.; Divita, G.; Johnson, L. N.; Endicott, J. A. *J. Biol. Chem.* **1999**, *274*, 8746.
47. Monks, A.; Scudiero, D.; Skehan, P.; Shoemaker, R.; Paull, K.; Vistica, D.; Hose, C.; Langley, J.; Cronise, P.; Vaigro-Wolff, A.; Gray-Goodrich, M.; Campbell, H.; Mayo, J.; Boyd, M. *J. Natl. Cancer Inst.* **1991**, *83*, 757.
48. Paull, K. D.; Shoemaker, R. H.; Hodes, L.; Monks, A.; Scudiero, D. A.; Rubinstein, L.; Plowman, J.; Boyd, M. R. *J. Natl. Cancer Inst.* **1989**, *81*, 1088.